Origin of the magnetoelectric couplings in the spin dynamics of molecular magnets

Sergio Leiva M.,[1,2,*] Sebastián A. Díaz,[3] and Alvaro S. Nunez[1,4]
[1]*Departamento de Física, FCFM, Universidad de Chile, 8370456 Santiago, Chile*
[2]*Institut für Physik, Martin-Luther-Universität Halle-Wittenberg, D-06099 Halle (Saale), Germany*
[3]*Faculty of Physics, University of Duisburg-Essen, D-47057 Duisburg, Germany*
[4]*Centro de nanociencia y nanotecnología CEDENNA, Avda. Ecuador 3493, Santiago, Chile*

(Received 28 November 2022; accepted 6 February 2023; published 1 March 2023)

We present a simple but attractive tool to describe and model the spin states of single molecule magnets. It is presented through a generalized Landau-Lifshitz-Gilbert equation with bias-dependent couplings that can be externally controlled. We provide a complete account of the various magnetic couplings [magnetic anisotropy, exchange, Dzyaloshinskii-Moriya interactions (DMI), damping, and magnetic noise's correlations] within a dimer of localized moments. The inversion symmetry breaking, ensued by the bias potential, induces a DMI between the magnetic elements that can be tuned accordingly. Through a calculation of the evolution of the spin, we conclude that such DMI is the dominant interaction during the reversal process. Along with the prescription to describe the time evolution of the spin moments, our results provide a qualitatively complete and integrated picture of various systems of interest in nanomagnetism.

DOI: 10.1103/PhysRevB.107.094401

I. INTRODUCTION

Magnetoelectric effects lie at the heart of the field of molecular spintronics [1]. They may well provide the ultimate tools required to garnish several applications [2]. The main goal being to furnish a powerful yet flexible control of magnets, it is attractive to couple them directly to electric fields. In this way, as it is expected, an increased but subtle control of otherwise unwieldy spin configurations will be achieved.

This work proposes an exploration into the magnetoelectric control of systems of localized moments such as those in single molecule magnets (SMM)[3]. We built upon previous results [4,5] to create an account of the dynamics of a simple molecular magnet, a spin dimer, acting as an electronic contact between two otherwise independent leads. We use a nonequilibrium formalism [6] in the description of the microscopic dynamics. From there, we arrive at an intuitive picture of the different mechanisms that affect the evolution of the localized moments' spin. Our results are encoded through a generalized form of the Landau-Lifshitz-Gilbert (LLG) equation. The usual form of the LLG equation has been used extensively in the treatment of atomistic models of magnetism, such as those devoted to the study of fast spin dynamics [7]. Different derivations of the LLG equation are applicable to SMM [8–11]. We show how, to satisfy internal consistencies demanded by the electrons' quantum mechanical behavior, it must be modified into a fully anisotropic and nonlocal framework. Starting from a toy-model based on itinerant electrons and localized spin moments, our calculations encompass complete derivations of the magnetic anisotropy, exchange (both isotropic and anisotropic), nonlocal and anisotropic damping, and fluctuations. We apply our theory to predict a voltage-induced Dzyaloshinskii-Moriya interaction (DMI) between the localized moments within dimer systems. The ultimate dependency of all these couplings on the bias voltage leads us to a form of voltage-controlled switching as expected from the literature [12,13]. Focusing on the inversion symmetry breaking, implied by the bias potential, we conclude that the DMI is an odd function of it and can be tuned accordingly. This DMI is restricted only to the nonequilibrium situation, vanishing when the bias voltage is turned off. We argue that such a coupling becomes dominant at the transition between the aligned and the antialigned configurations, dictating the course of the reversal process. We expect such a generalized LLG equation to become a pivotal ingredient in the analysis of the magnetic behavior of SMMs.

Aside from the semi-classical description just presented, it is interesting to wander into the quantum regime to see the profound implications that these findings might have [14]. Within this perspective, information is stored in the magnetic states of our dimer in the form of spin q-bits [15]. It has been reported that DMI provides a good source for entanglement [16] and opens up the possibilities of performing quantum processing tasks. Complementary, we can imagine the use of our proposal to induce entanglement in magnonic states. In this sense, it is well known that the DMI induces entangled states, as an antisymmetric exchange interaction [17,18]. Additionally, we mention that for certain 2D materials the DMI has been proven to promote topologically nontrivial magnonic states [19–21]. While our calculations are semi-classical and a full quantum treatment is beyond the scope of this paper, we expect that, our symmetry-based arguments and, hence, our results for the coupling constants will be qualitatively applicable as we approach the quantum domain.

*sergio-tomas.leiva-montecinos@physik.uni-halle.de

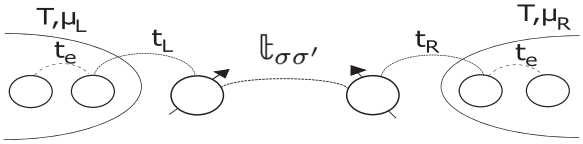

FIG. 1. Minimal model of two localized spins, $\mathbf{m}_1$ and $\mathbf{m}_2$, in between two semi-infinite leads characterized by their temperature T and chemical potential $\mu_{L/R}$, intrahopping t_e and contact hopping $t_{L/R}$, for left and right leads, respectively.

The molecular magnets we have in mind fit well within the ranges of other SMM reported in the experimental [22–26] and theoretical [27] literature. They have been proposed as magnetic memories and circuits [2,28,29] and can be integrated with other nanotechnological devices such as graphene-based hybrids [30]. Also, we found motivation in experiments that explore their potential in memories [31], in the proposal of using them in logic operations [32] and as exotic magnetic order such as toroidal configurations [33,34].

Concerning dimers, the subject we have chosen to apply the physical ideas of the paper, we can find various reports on the control of the relative spin orientation. Switching has been accomplished by using the mechanically controlled break-junction technique on two Co^{2+} ions [35]. Other theoretical works on dimer configuration are usually based upon the effects of ferromagnetic leads rather than normal metal leads [36,37].

II. MINIMAL MODEL OF A SPIN DIMER

We studied a toy model that consists of two leads and an electronic device as shown in Fig. 1. The device itself is composed of two sites, each one holding a spin. There are electronic hopping amplitudes both within the device and toward exterior leads represented as electronic reservoirs. This simple model provides a qualitatively compelling picture of various systems of interest in nanoscience. For instance, one might use it as a model of molecular magnet dimers, as we will do in the following. Additionally, we can apply it in the context of double quantum dots [38,39], spin-polarized STM [40], among others. Similar configurations have been studied in several reports [4,5,37,41–49], each one with their own particular focus and model features. Here we are interested in the nonequilibrium effects, i.e., the effects of a bias voltage across the device. We follow the framework presented in [4,5,50,51] to model this kind of systems.

In contrast with those works, we include a spin-dependent electronic hopping between the sites within the device. We include this hopping as a first approximation to represent the spin-orbit coupling in the electronic states within the molecule. The simplest way to study the effects of electrical current on an electronic device, down to the microscopic level, is by a one-dimensional tight binding model [52], in the nearest-neighbor approximation with a bias voltage. The first ingredients to analyze are the left and right leads, modeled as $\mathcal{H}_{L/R} = -t_e \sum_{\langle i,j\rangle,\sigma} c^\dagger_{L/R;i,\sigma} c_{L/R;j,\sigma}$, where t_e is the spin-independent hopping parameter within each lead. The operators $c^\dagger_{L(R);i,\sigma}$ and $c_{L(R);i,\sigma}$ represent the fermionic creation and annihilation operators in the left (right) lead, respectively.

The next contribution is the connection Hamiltonian that models the system-lead interaction by an electronic hopping between the rightmost (leftmost) site in the left (right) lead with the left (right) site of the electronic device, $\mathcal{H}_{(L/R)c} = -t_{L/R} \sum_\sigma (c^\dagger_{L/R,\sigma} c_{1/2,\sigma} + c^\dagger_{1/2,\sigma} c_{L/R,\sigma})$. Here t_L and t_R are the spin-independent hopping parameters quantifying the coupling between each lead and the system. In this case, $c^\dagger_{i,\sigma}$ and $c_{i,\sigma}$ represent the fermionic creation and annihilation operators in the device at site i. The interactions between the system and the environment can be separated into a purely electronic contribution along with a mixed one that combines the electronic and spin degrees of freedom, $\mathcal{H}_{\text{array}} = \mathcal{H}_e + \mathcal{H}_d$. The mixed Hamiltonian includes the Zeeman interaction and the $s-d$ interaction. Thus the electronic and mixed Hamiltonians are

$$\mathcal{H}_e = \epsilon_0 \sum_\sigma (c^\dagger_{1\sigma} c_{1\sigma} + c^\dagger_{2\sigma} c_{2\sigma}) + \sum_{\sigma,\sigma'} c^\dagger_{1\sigma} \mathbb{t}_{\sigma\sigma'} c_{2\sigma'} + \text{H.c.}, \tag{1}$$

$$\mathcal{H}_d = \mathcal{H}_0(\hat{\mathbf{S}}_1) + \mathcal{H}_0(\hat{\mathbf{S}}_2) - \Delta \hat{\mathbf{s}}_1 \cdot \hat{\mathbf{S}}_1 - \Delta \hat{\mathbf{s}}_2 \cdot \hat{\mathbf{S}}_2, \tag{2}$$

where $\hat{\mathbf{s}}_a = \frac{1}{2} \sum_{\sigma\sigma'} c^\dagger_{a\sigma} \boldsymbol{\tau}_{\sigma\sigma'} c_{a\sigma'}$ represents the electron's spin at site a, $c^\dagger_{a,\sigma}$, $c_{a,\sigma}$ are the fermionic creation and annihilation operators, and $\boldsymbol{\tau}_{\sigma\sigma'}$ is the vector containing the Pauli matrices. $\hat{\boldsymbol{S}}$ is the operator of the localized spin-S per site and Δ is local moment-electronic spin exchange coupling. Finally, $\mathcal{H}_0(\hat{\mathbf{S}}_a)$ and ϵ_0 represent all the spin and fermionic on-site energies due to the internal structure of the molecule, respectively, here we include magnetocrystalline anisotropic energies [3] and the Zeeman interaction with an external magnetic field in $\mathcal{H}_0(\hat{\mathbf{S}}_a)$. The definition of $\mathcal{H}_e$ in Eq. (1) includes the matrix $\mathbb{t}_{\sigma\sigma'} = t_0 \mathbb{1}_{\sigma\sigma'} + t\, \hat{\boldsymbol{t}} \cdot \boldsymbol{\tau}_{\sigma\sigma'}$, where $\mathbb{1}$ is the identity matrix and $\hat{\boldsymbol{t}}$ is a vector that sets the direction and strength of the spin orbit coupling (SOC). This constitutes a rudimentary form of SOC [53,54]. The election of this vector singles out the $\hat{\boldsymbol{t}}$ direction in the final emergent spin dynamics. The hopping strengths, t_0 and t, correspond to the spin-independent and spin-dependent hoppings, respectively.

III. EFFECTIVE MAGNETIC INTERACTIONS

A lengthy but straightforward analysis, based upon a detailed characterization of the electronic degrees of freedom [4,5] and a perturbative expansion on the local moment-electronic spin exchange coupling Δ was performed. It led us to the low-energy equations of motion within the semiclassical approximation for the spin variables (for a detailed exposition of such procedure, we refer the reader to Appendix A). The equation for the localized spin is

$$\frac{d\mathbf{m}_2}{dt} = \mathbf{m}_2 \times \left(\boldsymbol{H}_2 + \boldsymbol{\eta}_2 - \boldsymbol{\alpha}_{21} \frac{d\mathbf{m}_1}{dt} - \boldsymbol{\alpha}_{22} \frac{d\mathbf{m}_2}{dt} \right) \tag{3}$$

and a corresponding equation for $\mathbf{m}_1$ (exchanging indexes 1 and 2 throughout the expression). $\mathbf{m}_a$ is the direction of the spin at site a. This equation is quite similar to the Landau-Lifshitz-Gilbert equation. However, it presents certain peculiarities. First, we have defined the effective field $\boldsymbol{H}$ per site, which also depends on the orientation of the neighbor site, through what we identify as effective spin interactions.

It is important to emphasize that the overall behavior of the system is not dictated by a collective energy functional. Second, fluctuations due to interactions with itinerant electrons are accounted for in the vector field $\boldsymbol{\eta}_a$, called the stochastic magnetic field due to the way it enters in the equations and how it affects each localized spin directly. An important aspect of this stochastic field is that it is a consequence of the semiclassical approximation, so it is directly related to the system, within our approximations, rather than a phenomenological ingredient as often used in literature. Third, the damping is now nonlocal and nondiagonal, meaning that each spin affects the other one not only by the exchange interactions but also by interchanging energy. Even more, the damping has a preferred direction. All the above effective terms depend on the chemical potential of each lead, for which we use $\mu_L = \mu_F + \frac{eV}{2}$ and $\mu_L = \mu_F - \frac{eV}{2}$, so we now have the bias voltage V and the equilibrium chemical potential μ_F as external control parameters.

The effective field at site 2 is expressed by

$$\boldsymbol{H}_2 = -\frac{\partial \mathcal{E}_0}{\partial \mathbf{m}_2} + \Delta\langle \boldsymbol{s}_2\rangle + \Delta^2(J_2\mathbf{m}_1 + D_2\mathbf{m}_1 \times \hat{\boldsymbol{t}} + A_2(\mathbf{m}_1 \cdot \hat{\boldsymbol{t}})\hat{\boldsymbol{t}} + K_2(\mathbf{m}_2 \cdot \hat{\boldsymbol{t}})\hat{\boldsymbol{t}}) \tag{4}$$

and a corresponding equation for $\boldsymbol{H}_1$ (exchanging indexes 1 and 2 throughout the expression). In the first-order contribution, $O(\Delta)$, $\langle \boldsymbol{s}_2\rangle$ stands for the local electronic spin due to the effects of the SOC and the current flowing through the system, in absence of coupling with the localized moments. In the second-order terms $O(\Delta^2)$, the coefficient K_2 refers to a local anisotropy and A_2 to an anisotropic Ising exchange. J_2 stands for the usual isotropic exchange. Additionally, we have D_2, which sets the strength of the Dzyaloshinskii-Moriya interaction (DMI) between the two neighbors. This interaction favors an orthogonal configuration in the plane defined by the SOC's direction. Out of the usual symmetry arguments, the symmetric configuration at zero voltage is forced to show no DMI. It is only the inversion symmetry breaking provided by the bias voltage that allows the DMI to acquire a value different from zero. Indeed, as can be seen in Fig. 4 (lower panel), and as it is required by symmetry, the DMI strength is an odd function of the voltage and, hence, vanishes as the bias voltage is reduced to zero. The interaction shows the relation $D_2(V) = -D_2(-V)$, as well as, $D_2(V) = -D_1(V)$. This notion was put forward earlier [36] in a different model that involved SOC in the contacts rather than within the system.

In addition to the effective field, we have the effective damping matrix $\boldsymbol{\alpha}_{ab}$, which is very closely related to the second-order interactions. However, the matrix is, in general, not proportional to the identity, which means that the spin faces an anisotropic damping. We note that the effective damping mechanism is nonlocal. The dynamics of spin 1 affects spin 2 through $\boldsymbol{\alpha}_{12}$, and vice versa with $\boldsymbol{\alpha}_{21}$. The effective damping tensor is then expressed as

$$\boldsymbol{\alpha}_{ab} = \Delta^2\big(\alpha_{ab}^{(i)}\mathbb{1} + \alpha_{ab}^{(an)}\hat{\boldsymbol{t}} \otimes \hat{\boldsymbol{t}}\big), \tag{5}$$

where $\otimes$ stands for outer multiplication. As it is made explicit in the last expression, the dissipation is naturally separated into isotropic and anisotropic damping, however, from the analytical calculations we would also have an antisymmetric damping which for our analysis is discarded due to the small numerical value relative to the other components of the tensor. The first coefficient $\alpha_{ab}^{(i)}$, also know as Gilbert damping, forces the spins to align with the effective field. However, even though the second coefficient $\alpha_{ab}^{(an)}$ acts as a damping factor perpendicular to the time derivative of the spin, it can also be interpreted as new field in the SOC direction.

Similarly to the damping tensor, the correlations of the field $\boldsymbol{\eta}$ also have two components called symmetric and anisotropic correlation strengths. Nevertheless, in contrast with $\boldsymbol{\alpha}$, the antisymmetric part is identically zero due to the symmetries of the model and its electronic structure. The correlation functions are represented by

$$\langle \boldsymbol{\eta}_a(t)\boldsymbol{\eta}_b(t')\rangle = \Delta^2\big(j_{ab}^{(i)}\mathbb{1} + j_{ab}^{(an)}\hat{\boldsymbol{t}} \otimes \hat{\boldsymbol{t}}\big)\delta(t-t'). \tag{6}$$

In particular, the spin-orbit induced torques act together with stochastic fields whose statistical features are affected by the SOC and are themselves anisotropic in nature. On one hand, they include the previously reported [4,5] isotropic contribution $j_{ab}^{(i)}$ to the correlations. However, $j_{ab}^{(an)}$ is something exclusively related to the SOC and introduces an important feature in the equations. Its explicit dependence on the SOC direction emerges via the anisotropic correlation factor and changes the otherwise spherically distributed noise contribution.

Equations (3) to (6), encapsulate the main results of the present work. They provide a minimal model to handle localized moments interacting with electrons undergoing SOC. Along with the effective interactions $\{J_{1,2}, D_{1,2}, A_{1,2}, K_{1,2}\}$ and the damping factors $\{\alpha_{ab}^{(i)}, \alpha_{ab}^{(an)}\}$, it includes a prescription to evaluate the time evolution of the localized moments. The coefficients are calculated from the family of electronic Green's functions. The details of this procedure are shown in the Appendix A. In the evaluation of the effective interactions, damping coefficients and correlation strengths, we use the parameters $t_e = 100\,\text{meV}$, $t_0 = 2\,\text{meV}$, $t_L = t_R = 10\,\text{meV}$, and the on-site energies were taken as $\epsilon_0 = 0\,\text{meV}$, however, a difference in the on-site energy of each site can be used as control parameters [37]. A selection of the couplings is represented in Fig. 2 for a weak SOC regime, $t = 5\%t_0$, while a more thorough characterization is provided in Appendix B. Throughout the calculations we considered $T \sim 0\,\text{K}$, although a nonzero temperature and even a temperature gradient can readily be included in our model, opening a path toward magnetothermal effects [45].

IV. DYNAMICS WITH ONE SPIN PINNED

We pursue the application of the ideas above through a detailed analysis of a particular case. We study the situation where one of the localized spins is pinned, so $\mathbf{m}_1$ is pointing along a constant fixed direction, while $\mathbf{m}_2 = \mathbf{m}$, undergoes the dynamics prescribed by the previous section. As it turns out, we can define the effective energy for the free spin as

$$\mathcal{E}_{\mathbf{m}_1,t}(\mathbf{m}) = \mathcal{E}_0(\mathbf{m}) - \Delta\langle \boldsymbol{s}\rangle \cdot \mathbf{m} - \Delta^2\big[J\mathbf{m}\cdot\mathbf{m}_1 + D\hat{\boldsymbol{t}}\cdot(\mathbf{m}\times\mathbf{m}_1) + A(\mathbf{m}\cdot\hat{\boldsymbol{t}})(\mathbf{m}_1\cdot\hat{\boldsymbol{t}}) + \tfrac{1}{2}K(\mathbf{m}\cdot\hat{\boldsymbol{t}})^2\big]. \tag{7}$$

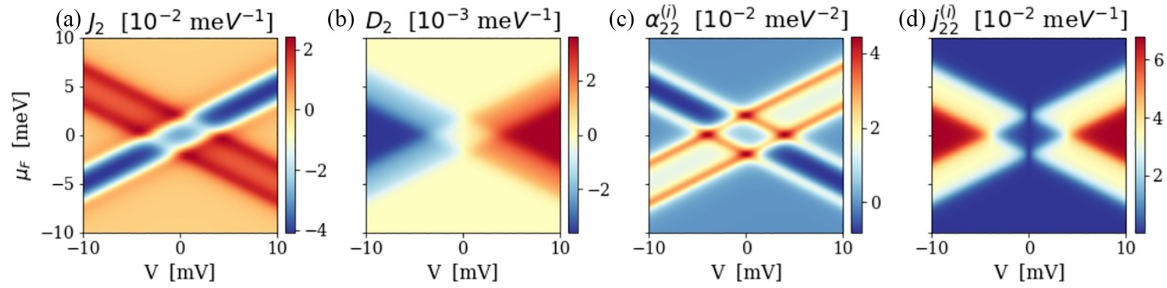

FIG. 2. Selected voltage-induced effective magnetic interactions and damping coefficient of the spin dimer. (a) The effective symmetric interaction J_2. The system presents a preferred antiferromagnetic configuration ($J_2 < 0$) for a narrow band delimited approximately by $|\mu_R| < t_0 - t$, while for other relations of μ_F and V, the system prefers a ferromagnetic configuration ($J_2 > 0$) in an x-like behavior. (b) The effective DMI D_2. The DMI presents a steplike behavior, where the thickness of the first plateau is controlled by the intensity of the SOC, this is approximately bounded by $|\mu_{R/L}| < t_0 - t$. The interaction shows the relation $D_2(V) = -D_2(-V)$, as well as, $D_2(V) = -D_1(V)$. Both of which are consistent with the broken inversion symmetry in the system. (c) The effective Gilbert damping $\alpha_{22}^{(i)}$. The maxima of the damping are approximately at $|\mu_L| = t_0 - t$ and $|\mu_R| = t_0$. The Gilbert damping can represent an energy injection for $|\mu_L| < t_0 - t$ and $|\mu_R| > t_0$. (d) The isotropic component of the correlation function $j_{22}^{(i)}$ presents a steplike structure delimited by the same x-like lines as for the symmetric interaction.

Hereafter, for notational convenience, we have dropped the indexes in the different couplings, damping components, and correlation factors. With this expression of the energy, we can come back to equation (3) and write the equation of motion for the free spin under the effects of the leads and the interaction with the fixed spin. The final equation of motion reads

$$\frac{d\mathbf{m}}{dt} = \mathbf{\Gamma}_{\text{eff}} + \mathbf{\Gamma}_{\text{noise}} + \mathbf{\Gamma}_d^{(\text{i})} + \mathbf{\Gamma}_d^{(\text{an})}, \tag{8}$$

where $\mathbf{\Gamma}_{\text{eff}}$ corresponds to the torque from the effective fields, $\mathbf{\Gamma}_{\text{noise}} = \mathbf{m} \times \boldsymbol{\eta}$ is the stochastic torque, while $\mathbf{\Gamma}_d^{(\text{i})} = \alpha^{(i)}\mathbf{m} \times \frac{d\mathbf{m}}{dt}$ and $\mathbf{\Gamma}_d^{(\text{an})} = \alpha^{(an)}(\hat{\boldsymbol{t}} \cdot \frac{d\mathbf{m}}{dt})\mathbf{m} \times \hat{\boldsymbol{t}}$ correspond to the torques with origin in the damping mechanisms. See Fig. 3. Equation (8) corresponds to an anisotropic stochastic Landau-Lifshitz-Gilbert equation, other extensions of this equation has been studied in Refs. [55,56].

We study two approaches to solve Eq. (8). First, by a direct statistical analysis by means of the implicit stochastic Euler method. This approach was sufficient to integrate the problem, for all the parameter values studied in the present work. We find that the effective field acting on the spin is the sum of two contributions, $\mathbf{\Gamma}_{\text{eff}}$ and $\mathbf{\Gamma}_d^{(\text{an})}$, since the latter gives rise to both field and dampinglike torques. We identify the this extra contribution as a spin-orbit induced torque [57].

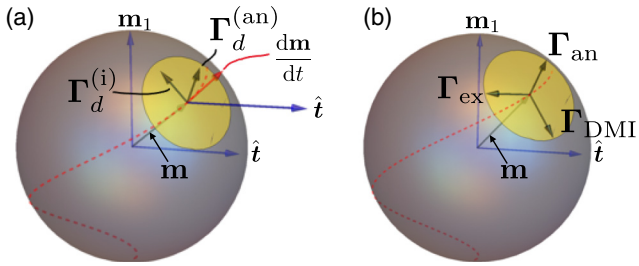

FIG. 3. Torques acting on the free spin of the dimer. The other spin is pinned along the fixed direction $\mathbf{m}_1$. The direction of the free spin and the SOC are $\mathbf{m}$ and $\hat{\boldsymbol{t}}$, respectively. (a) Orientation of the dissipative torques $\mathbf{\Gamma}_d^{(\text{i})}$ and $\mathbf{\Gamma}_d^{(\text{an})}$. The dashed red line corresponds to a possible trajectory of the localized spin orientation. At a certain instant, we evaluate $d\mathbf{m}/dt$ (red arrow). (b) The torque from the effective field, $\mathbf{\Gamma}_{\text{eff}}$, can be split as a sum of $\mathbf{\Gamma}_{\text{ex}}$, originated in the exchange coupling, $\mathbf{\Gamma}_{\text{an}}$ from the anisotropy contributions and $\mathbf{\Gamma}_{\text{DMI}}$ stemming from the DMI. All torques lie within the tangent plane to the sphere, a section of which we have illustrated with the yellow circle.

The direct solutions of the Langevin equation, although reliable, take a considerable computational effort, even in the case of small systems. For this reason, we have complemented our results with a second alternative, faster albeit only approximately accurate, for the determination of the expectation values using approximate solutions to the Fokker-Planck (FP) equation [58]. In this way, we can obtain the mean orientation of the spin for each value of the bias voltage. In a weak SOC regime, $t = 5\%t_0$, for the probability density on the sphere, $\mathcal{P}(\mathbf{m})$, the approximate solution corresponds to the suggestive result $\mathcal{P}(\mathbf{m}) \propto \exp(-\beta\mathcal{E}_{\mathbf{m}_1,t}(\mathbf{m}))$, where we have defined the effective temperature T_{eff} as $\beta = 1/k_B T_{\text{eff}} = 2S^2\hbar\alpha^{(i)}/j^{(i)}$. We highlight the simple relation for the effective temperature of the system, that sets the strength of the spin fluctuations as function of voltage. This result is in agreement with the stochastic switching between two opposite magnetization states reported in the literature [59].

As illustrated in Fig. 4, the system can present both antiferromagnetic, $\mathbf{m}_z \sim -S$, or ferromagnetic, $\mathbf{m}_z \sim S$, configurations upon different bias voltage. It is clear that the antiferromagnetic configuration has a switching point when we increase (reduce) the voltage from 0 to 3 mV (-3 mV), value at which the system now prefers a ferromagnetic configuration. This can be explained by the more energetic itinerant electrons scattering into the dimer, and deduced from the decrease of the dominant interaction, J_2. Additionally, Fig. 4 also shows that the out-of-plane component $\mathbf{m}_y$ dominates over a small window nearby the switching point. It can be seen that for opposite bias its direction is reversed. We conclude that the emergent DMI dominates the course of the reversal process. This feature is a direct and measurable consequence of the emergent DMI.

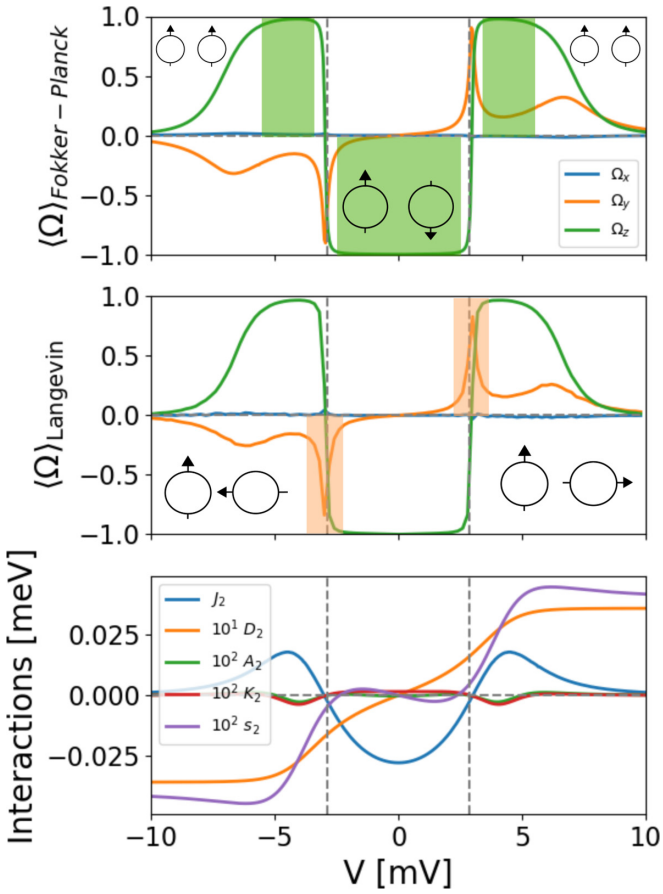

FIG. 4. Average value of the unpinned localized spin's direction for each Cartesian component, using the FP method (top), the Langevin method (middle), and the relative comparison of the effective interactions (bottom). We have denoted $\mathbf{\Omega} = \mathbf{m}/S$ and use $\mathbf{m}_1 = \hat{z}$ and $\hat{\boldsymbol{t}} = \hat{\boldsymbol{x}}$. The calculation was done for $\mu_F = 0$ meV, $S = 5/2$, $T = 0$ K, $t = 0.05$ meV, and the same values used in Ref. [5] for the Zeeman interaction and the mangetocrystalline anisotropic constant for easy-axis and in-plane anisotropies. We can see that the system presents a stable antiferromagnetic configuration for low bias voltage up to approximately ± 3 mV, after which the system reverses the magnetization to a ferromagnetic configuration, both highlighted in green in the top panel. However, it is interesting to note that the reversal process is dominated by the DMI interaction at around ± 3 mV, $D_2 > J_2$ which allows the system to reverse the magnetization in a controlled manner, highlighted in orange in the middle panel.

V. CONCLUSIONS

We presented a derivation of the low-energy semiclassical behavior of a symmetric dimer system of localized moments in contact with a nonequilibrium electronic bath. This approach provides a qualitatively complete picture of various systems of interest in nanoscience. For example, it might be used as a model of molecular magnet dimers or one can envision its application in the context of double quantum dots [38,39], spin-polarized STM [40], among others. With minor modifications, our conclusions can be applied to those experimental setups. We used a semiclassical nonequilibrium formalism in the description of the microscopic dynamics that guided us towards an effective behavior for the localized spins. The analysis relies on a second-order expansion in the localized moment-electronic spin exchange coupling. From it, we derived an intuitive picture of the different mechanisms that affect the evolution of the localized moments' spin. Our analysis required a complete derivation of a generalized form of the Landau-Lifshitz-Gilbert equation, including magnetic anisotropy, isotropic and anisotropic exchange, and a voltage-induced DMI. The dynamics is complemented by anisotropic and nonlocal damping coefficients and, correspondingly, anisotropic fluctuating torques with nonlocal correlations. We anticipate this generalized equation to become a key ingredient of magnetic simulations in the context of complex SMMs. Additionally, we found that the external bias voltage affects each interaction's strength. In this way, the exchange interaction can be tuned, with the aid of the bias voltage, from antiferromagnetic to ferromagnetic. The inversion symmetry breaking implied by the bias potential induces a DMI between the magnetic elements that can be tuned accordingly. This voltage-induced DMI is the dominating torque during the reversal process. It selects the reversion path followed by the local moments. We expect that these results might prove useful even when taken to the quantum regime, where they can be expected to aid in the electrical control of entanglement properties.

ACKNOWLEDGMENTS

A.S.N. and S.L.M. thank E. Aguilera, R. Jaeschke, A. Mella, and A. O. Leon for useful discussions and insightful comments throughout this work. Funding is acknowledged from Fondecyt Regular 1190324, and Financiamiento Basal para Centros Científicos y Tecnológicos de Excelencia AFB220001. Powered@NLHPC: This research was partially supported by the supercomputing infrastructure of the NLHPC (ECM-02).

APPENDIX A: ELECTRONIC GREEN'S FUNCTIONS CALCULATIONS

To include the nonequilibrium effects of the electrical current, we use the Keldysh formalism to model the system [6]. The total action $\mathcal{S}_T$, can be separated into an electronic action $\mathcal{S}_\Psi$, an spin action $\mathcal{S}_{\boldsymbol{m}}$ and interaction action $\mathcal{S}_I$, where each term is written as

$$S_{\boldsymbol{m}} = \sum_a \int_{\mathcal{C}'} dt_c \left[-\hbar S \frac{d\omega_a}{dt_c} + \mathbf{m}_a \cdot \boldsymbol{h} - \mathcal{E}[\mathbf{m}_a] \right], \quad \text{(A1)}$$

$$S_\Psi = \int_{\mathcal{C}'} dt_c \left[i\hbar \sum_{\sigma,i} (\psi^*_{Li,\sigma} \partial_{t_c} \psi_{Li,\sigma} + \psi^*_{Di,\sigma} \partial_{t_c} \psi_{Di,\sigma} + \psi^*_{Ri,\sigma} \partial_{t_c} \psi_{Ri,\sigma}) - H_R - H_L - H_{Rc} - H_{Lc} - H_e \right], \quad \text{(A2)}$$

$$S_I = \sum_a \int_{\mathcal{C}'} dt_c \Delta \boldsymbol{m}_a \cdot \boldsymbol{s}_a, \quad \text{(A3)}$$

where, in the action for the localized spins $\mathcal{S}_{\boldsymbol{m}}$, ω_a is the Berry phase for the spin variable [60], and in the action for the free or itinerant electrons $\mathcal{S}_\Psi$, the terms with contour-time derivative, $\psi^*\partial_{t_c}\psi$, are the Berry phases of the Grassmann fields [61], and $\boldsymbol{m}_a$ is the direction of the spin at site a. Here we can expand up to second order in the *s-d* interaction factor Δ and take the low-energy limit to explore the spin dynamics of each localized spins.

From the expression of the total action $S_T = S_{\boldsymbol{m}} + S_\Psi + S_I$, we can construct the nonequilibrium path integral over the Keldysh contour. This can be calculated following the work presented in Ref. [5], however, here we present the additional steps to extend their results for the present work. First we need to integrate the electronic degree of freedom, but due to the interacting action S_I we need to expand up to second order in the *s-d* interaction factor Δ. A common way yo expand it is by using the Cumulant expansion [58], where we obtain the integral Kernel

$$K^{ij}_{ab}(t_c, t_c') \equiv \frac{i}{2\hbar}\left[\left\langle \mathcal{T} s^i_a(t_c) s^j_b(t_c')\right\rangle - \left\langle s^i_a(t_c)\right\rangle\left\langle s^j_b(t_c')\right\rangle\right]. \tag{A4}$$

So the effective action up to second order in Δ is

$$\mathcal{S} = \mathcal{S}_{\boldsymbol{m}} + \int_{\mathcal{C}_t} dt' (S\Delta \sum_a \mathbf{m}_a \cdot \langle \boldsymbol{s}_a(t')\rangle + \int_{\mathcal{C}_t} dt'' \Delta^2 \sum_{ij,ab} \boldsymbol{m}^i_a(t') K^{ij}_{ab}(t', t'') \boldsymbol{m}^j_b(t'')). \tag{A5}$$

The expression of the integral kernel in eEq. (A4) can be expressed in terms of a electronic Green functions $iG_{a\sigma;b\sigma'}(t,t') \equiv \langle \mathcal{T}\psi_{a\sigma}(t)\psi^*_{b\sigma'}(t')\rangle$ with the aid of the Wick theorem, as

$$K^{ij}_{ab}(t,t') \equiv \frac{i}{8\hbar}\sum_{\sigma\sigma'\mu\mu'} \tau^i_{\sigma\sigma'}\tau^j_{\mu\mu'} G_{a\sigma';b\mu}(t,t') G_{b\mu';a\sigma}(t',t). \tag{A6}$$

This expression is customarily associated with a bubble diagram

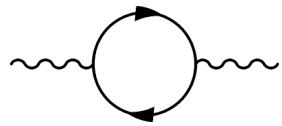

With that, we can calculate the energy representation using electronic transport theory [62]. So we obtain the energy representation of the dimer kernel in terms of the electronic Green's function (GF) components.

$$K^{ij(\pm)}_{ab}(\epsilon) = \frac{-1}{8}\sum_{\sigma\sigma'\mu\mu'} \tau^i_{\sigma\sigma'}\tau^j_{\mu\mu'} \int \frac{d\epsilon'}{2\pi}\frac{d\epsilon''}{2\pi} \frac{G^>_{a\sigma';b\mu}(\epsilon') G^<_{b\mu';a\sigma}(\epsilon'') - G^<_{a\sigma';b\mu}(\epsilon') G^>_{b\mu';a\sigma}(\epsilon'')}{\epsilon^\pm - \epsilon' + \epsilon''}, \tag{A7}$$

$$K^{ij(K)}_{ab}(\epsilon) = -\frac{i\pi}{4}\sum_{\sigma\sigma'\mu\mu'} \tau^i_{\sigma\sigma'}\tau^j_{\mu\mu'} \int \frac{d\epsilon'}{2\pi}\frac{d\epsilon''}{2\pi} \delta(\epsilon - \epsilon' + \epsilon'')[G^>_{a\sigma';b\mu}(\epsilon') G^<_{b\mu';a\sigma}(\epsilon'') + G^<_{a\sigma';b\mu}(\epsilon') G^>_{b\mu';a\sigma}(\epsilon'')]. \tag{A8}$$

The electronic GF can be calculated from the advanced and retarded GF that contemplates the self-energies of two semiinfinite leads. However, now we need a connection between the lesser and greater GF, and the advanced and retarded GF. From the electronic Green's function that contemplate both site and spin, we now have a nondiagonal matrix in spin for the advanced and retarded GF of the form:

$$G^{(\pm)}_{a\sigma;b\sigma'}(\epsilon) = G^{(s)(\pm)}_{ab}(\epsilon)\mathbb{I}_{\sigma\sigma'} + G^{(t)(\pm)}_{ab}(\epsilon)[\hat{\boldsymbol{t}}\cdot\boldsymbol{\tau}]_{\sigma\sigma'}, \tag{A9}$$

where we define the *singlet* function $G^{(s)(\pm)}_{ab}(\epsilon)$ due to be related to the symmetric part in spin space, and the *triplet* function $G^{(t)(\pm)}_{ab}(\epsilon)$ due to the trace-less part of the full electronic GF in spin space. The matrix components of the *singlet* functions are

$$G^{(\pm)(s)}_{11}(\epsilon) = \frac{g^\pm_2}{2}\left[\frac{1}{g^\pm_1 g^\pm_2 - (t_0+t)^2} + \frac{1}{g^\pm_1 g^\pm_2 - (t_0-t)^2}\right], \tag{A10}$$

$$G^{(\pm)(s)}_{12}(\epsilon) = G^{(\pm)(s)}_{21}(\epsilon) = -\frac{1}{2}\left[\frac{t_0+t}{g^\pm_1 g^\pm_2 - (t_0+t)^2} + \frac{t_0-t}{g^\pm_1 g^\pm_2 - (t_0-t)^2}\right], \tag{A11}$$

$$G^{(\pm)(s)}_{22}(\epsilon) = \frac{g^\pm_1}{2}\left[\frac{1}{g^\pm_1 g^\pm_2 - (t_0+t)^2} + \frac{1}{g^\pm_1 g^\pm_2 - (t_0-t)^2}\right], \tag{A12}$$

and of the triplet functions:

$$G^{(\pm)(t)}_{11}(\epsilon) = \frac{g^\pm_2}{2}\left[\frac{1}{g^\pm_1 g^\pm_2 - (t_0+t)^2} - \frac{1}{g^\pm_1 g^\pm_2 - (t_0-t)^2}\right], \tag{A13}$$

$$G_{12}^{(\pm)(t)}(\epsilon) = G_{21}^{(\pm)(t)}(\epsilon) = -\frac{1}{2}\left[\frac{t_0 + t}{g_1^{\pm} g_2^{\pm} - (t_0 + t)^2} - \frac{t_0 - t}{g_1^{\pm} g_2^{\pm} - (t_0 - t)^2}\right], \tag{A14}$$

$$G_{22}^{(\pm)(t)}(\epsilon) = \frac{g_1^{\pm}}{2}\left[\frac{1}{g_1^{\pm} g_2^{\pm} - (t_0 + t)^2} - \frac{1}{g_1^{\pm} g_2^{\pm} - (t_0 - t)^2}\right], \tag{A15}$$

where we have define $g_i^{\pm}(\epsilon) \equiv \epsilon - \hbar\Sigma_i^{\pm}(\epsilon)$, with the retarded and advanced self-energies of a semi-infinite lead $\Sigma^{\pm}(\epsilon)$. By using the steady-state kinetic equation [5,62,63], we obtain that the lesser and greater GF are

$$G^{\lessgtr}(\epsilon) = G^{(+)}(\epsilon)\hbar\Sigma^{\lessgtr}(\epsilon)G^{(-)}(\epsilon), \tag{A16}$$

with the aid of the *in and out-scattering* function $\Sigma^{\lessgtr}$. Replacing Eq. (A9) in Eq. (A16), we get a similar decomposition in singlet and triplet GF for the lesser and greater components,

$$G^{\lessgtr}_{a\sigma;b\sigma'}(\epsilon) = G^{(s)\lessgtr}_{ab}(\epsilon)\mathbb{I}_{\sigma\sigma'} + G^{(t)\lessgtr}_{ab}(\epsilon)[\hat{\boldsymbol{t}}\cdot\boldsymbol{\tau}]_{\sigma\sigma'}, \tag{A17}$$

where we have define the lesser and greater, singlet function and triplet function as

$$G^{(s)\lessgtr}_{ab} = \sum_c \left[G^{(s)(+)}_{ac}\hbar\Sigma^{\lessgtr}_c G^{(s)(-)}_{cb} + G^{(t)(+)}_{ac}\hbar\Sigma^{\lessgtr}_c G^{(t)(-)}_{cb}\right],$$

$$G^{(t)\lessgtr}_{ab} = \sum_c \left[G^{(s)(+)}_{ac}\hbar\Sigma^{\lessgtr}_c G^{(t)(-)}_{cb} + G^{(t)(+)}_{ac}\hbar\Sigma^{\lessgtr}_c G^{(s)(-)}_{cb}\right]$$

with these expressions we can come back to the

$$\mathbb{G}^{\{p,q\}}_{ab\pm}(\epsilon', \epsilon'') \equiv G^{(p)>}_{ab}(\epsilon')G^{(q)<}_{ba}(\epsilon'') \pm G^{(p)<}_{ab}(\epsilon')G^{(q)>}_{ba}(\epsilon''). \tag{A18}$$

Furthermore, we actually see that both expressions has only three very characteristic relations between the vector indices. The advanced and retarded components can be written as

$$K^{ij(\pm)}_{ab}(\epsilon) = -\frac{1}{4\hbar}\int \frac{d\epsilon'}{2\pi}\frac{d\epsilon''}{2\pi}\frac{1}{\epsilon^{\pm} - \epsilon' + \epsilon''} \times [\mathcal{J}_{ab}(\epsilon', \epsilon'')\delta^{ij} + i\mathcal{D}_{ab}(\epsilon', \epsilon'')\epsilon^{ijk}\hat{t}^k + 2\bar{\Gamma}_{ab}(\epsilon', \epsilon'')\hat{t}^i\hat{t}^j], \tag{A19}$$

where

$$\mathcal{J}_{ab}(\epsilon', \epsilon'') = \mathbb{G}^{\{s,s\}}_{ab(-)}(\epsilon', \epsilon'') - \mathbb{G}^{\{t,t\}}_{ab(-)}(\epsilon', \epsilon''), \tag{A20}$$

$$\mathcal{D}_{ab}(\epsilon', \epsilon'') = \mathbb{G}^{\{s,t\}}_{ab(-)}(\epsilon', \epsilon'') - \mathbb{G}^{\{t,s\}}_{ab(-)}(\epsilon', \epsilon''), \tag{A21}$$

$$\bar{\Gamma}_{ab}(\epsilon', \epsilon'') = \mathbb{G}^{\{t,t\}}_{ab(-)}(\epsilon', \epsilon''). \tag{A22}$$

Here we clearly anticipate that $\mathcal{J}_{ab}$, $\mathcal{D}_{ab}$, $\bar{\Gamma}_{ab}$ will give the effective symmetric exchangelike interaction, the effective antisymmetric exchangelike interaction and an effective anisotropic-like interaction, respectively. Analogously for the Keldysh component in (A8), we find

$$K^{ij(K)}_{ab}(\epsilon) = -\frac{i\pi}{2\hbar}\int \frac{d\epsilon'}{2\pi}\frac{d\epsilon''}{2\pi}\delta(\epsilon - \epsilon' + \epsilon'') \times [\bar{j}_{ab}(\epsilon', \epsilon'')\delta^{ij} + i\bar{d}_{ab}(\epsilon', \epsilon'')\epsilon^{ijk}\hat{t}^k + 2\bar{g}_{ab}(\epsilon', \epsilon'')\hat{t}^i\hat{t}^j], \tag{A23}$$

where we define $\bar{j}_{ab}$, $\bar{d}_{ab}$, and $\bar{g}_{ab}$ by the same structure as for $\{\mathcal{J}_{ab}, \mathcal{D}_{ab}, \bar{\Gamma}_{ab}\}$, but replacing $(-) \mapsto (+)$ in (A18). Now that we have make the connection of the advanced, retarded and Keldysh components to the singlet and triplet advanced and retarded electronic Green's functions, we can perform a Taylor expansion for $\epsilon \sim 0$ up to first order, and find that the zeroth-order term is related to the interactions $(J_{ab}, iD_{ab}, \Gamma_{ab})$ and the first-order part is related to the dampings $(\alpha_{ab}, \gamma_{ab})$. Analogously, for the correlation factors, we find that only the

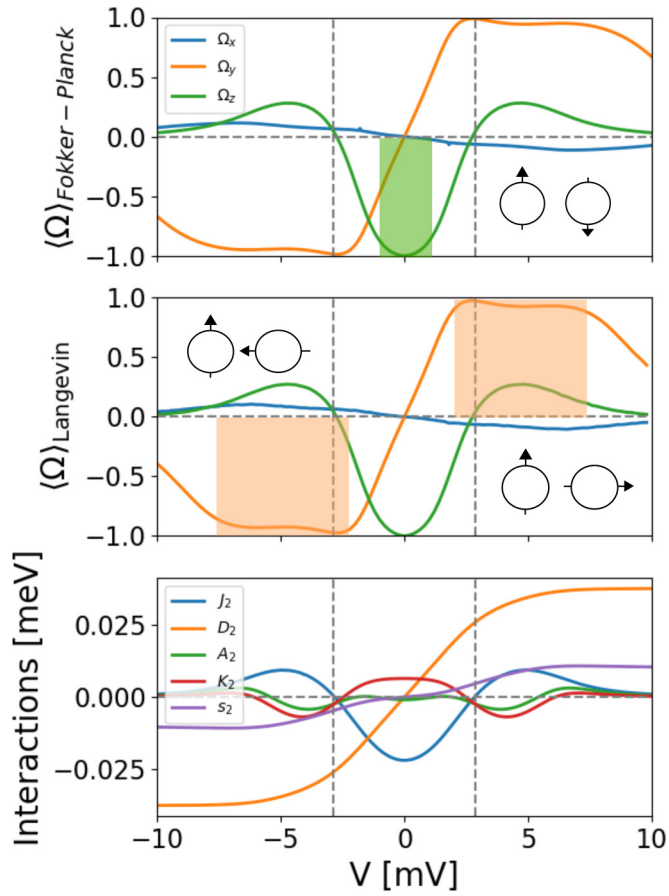

FIG. 5. Average value of the unpinned localized spin's direction for each Cartesian component, using FP method (top) and the Langevin method (middle), and the relative comparison of the effective interactions (bottom). We have denoted $\boldsymbol{\Omega} = \mathbf{m}/S$ and $\mathbf{m}_1 = \hat{\boldsymbol{k}}$. The calculation was done for $\mu_F = 0$ meV, $S = 5/2$, $T = 0$ K, $t = 1$ meV, and the same values used in Ref. [5] for the Zeeman interaction and the mangetocrystalline anisotropic constant for easy-ayis and in-plane anisotropies. In this case, only the antiferromagnetic configuration is preserved since the DM interaction overcomes the isotropic interaction before the switching voltage. Therefore the equilibrium orientation is now orthogonal to the pinned spin. In this case, we still can control the equilibrium configuration but without having a parallel configuration.

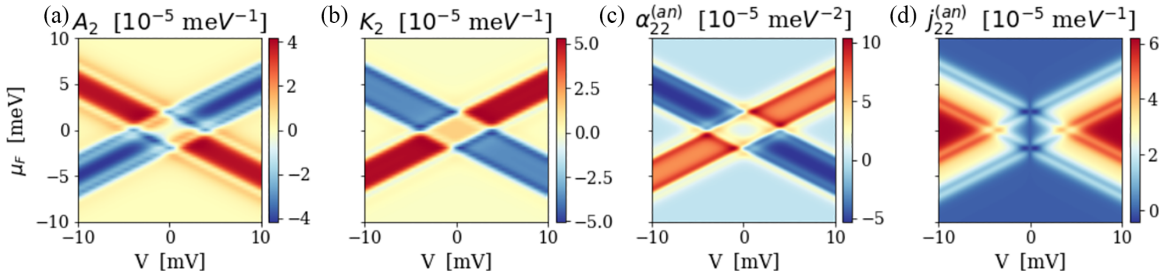

FIG. 6. Selected voltage-induced effective magnetic interactions and damping coefficient of the spin dimer. The anisotropic Ising exchange (a) and the local anisotropy (b), both resemblance the strucutre of the symmetric interaction, however they are several orders of magnitude smaller than J_2, even though, A_2 presents extra resonance lines associated to a splitting due to the SOC. The local anisotropy present the opposite sign for the same set of parameters, which we associate to an inercia component since it only react to the alignment of the free spin and the SO vector $\hat{\boldsymbol{t}}$ and it oppose the change of the other interactions. The anisotropic damping (c) and the anisotropic correlation component (d) show the same behavior as their isotropic counterparts but, as for A_2, they present a splitting in the lines that dictate the maxima due to the SOC.

zeroth order is nonzero and sufficient to study the system under our assumptions. For the case of one spin fixed, only a few components are relevant for the equation of motion of the free spin.

$$(J_{21}, iD_{21}, \Gamma_{21}, \Gamma_{22}) = -\frac{1}{2}\int \frac{d\epsilon'}{2\pi}\frac{d\epsilon''}{2\pi}\frac{1}{\epsilon'' - \epsilon' + i\delta}(\mathcal{J}_{21}, i\mathcal{D}_{21}, \bar{\Gamma}_{21}, \bar{\Gamma}_{22})(\epsilon', \epsilon''),$$

$$(\alpha_{22}, \gamma_{22}) = -\frac{1}{4}\int \frac{d\epsilon'}{2\pi}\frac{\partial}{\partial\epsilon}\big((\mathcal{J}_{22}, \bar{\Gamma}_{22})(\epsilon', \epsilon + \epsilon')\big), \quad i\beta_{22} = -\frac{1}{2}\int \frac{d\epsilon'}{2\pi}\frac{d\epsilon''}{2\pi}\mathcal{P}\left(\frac{\frac{\partial}{\partial\epsilon''}[i\mathcal{D}_{22}(\epsilon', \epsilon'')]}{\epsilon'' - \epsilon'}\right),$$

$$(j_{22}, g_{22}) = -\frac{i}{4\hbar}\int \frac{d\epsilon'}{2\pi}(\bar{j}_{22}, \bar{g}_{22})(\epsilon', \epsilon'), \quad id_{22} = 0, \quad \langle \boldsymbol{s}_a(t)\rangle = Si\hat{\boldsymbol{t}}G_{aa}^{(t)}(t, t). \tag{A24}$$

For simplicity in the notation, throughout the text, we replace the effective factors indices as $\hbar\{J_{12}, J_{21}\} \to \{J_1, J_2\}$, $i\hbar\{D_{12}, D_{21}\} \to \{D_1, D_2\}$, $2\hbar\{\Gamma_{12}, \Gamma_{21}\} \to \{A_1, A_2\}$, $2\hbar\{\Gamma_{11}, \Gamma_{22}\} \to \{K_1, K_2\}$, $\hbar\{\alpha_{21}, \alpha_{22}\} \to \{\alpha_1^{(i)}, \alpha_2^{(i)}\}$, $\hbar\{\gamma_{21}, \gamma_{22}\} \to \{\alpha_1^{(an)}, \alpha_2^{(an)}\}$, $\hbar\{j_{21}, j_{22}\} \to \{j_1^{(i)}, j_2^{(i)}\}$, and $\hbar\{g_{21}, g_{22}\} \to \{j_1^{(an)}, j_2^{(an)}\}$.

APPENDIX B: EVALUATION OF THE EFFECTIVE COUPLING, DAMPING AND CORRELATIONS

The numerical values of the effective factors can be calculated with the corresponding expression in Eq. (A24). In Fig. 2, we show the symmetric and DM interaction, as well as the Gilbert damping and the isotropic component of the correlation function. Now we can see the numerical values of the local and Ising anisotropies, and the anisotropic damping and component of the correlation function in Fig. 6. We can see the resemblance of the anisotropic interactions, A_2 and K_2, with the symmetric interaction J_2 in the x-like structure, however the anisotropic interactions are very weak as we can see in bottom part of Fig. 4. This explain why, even though we have torques that would shift the equilibrium orientation from the z direction ($\hat{\boldsymbol{m}}_1$ direction), we still see that for low enough voltages the equilibrium configuration is parallel or antiparallel to the pinned spin. It is interesting to notice that, for most parameter configurations, the local anisotropic interaction has an opposite sign compared with the isotropic and anisotropic Ising interaction. Since K_2 is only sensitive to the orientation of the free spin, we identify it as a self-interaction and can be interpreted as an inercia factor, due to the opposition to the change in orientation.

The anisotropic damping and correlection factor presents similar structure as their isotropic counterparts, with the addition of extra local maxima lines. This splitting of the local maxima is induced from the SOC, that modify the lines as for the DM interaction. As for the anisotropic interactions, $\alpha_{22}^{(an)}$ and $j_{22}^{(an)}$, are several orders of magnitude smaller than $\alpha_{22}^{(i)}$ and $j_{22}^{(i)}$, from which we expect a low effect in the damping and correlation function. This, however, has a more important effect for the inversion process as well as with the DMI compared with J_2 for those voltages.

However, for completeness we also study the dependence upon a stronger SOC strength for the aforementioned effective factors, as well as for the numerical solution of the Langevin and Fokker-Planck equation. Therefore here we include what we call strong SOC case, i.e., $t = 0.5t_0$, shown in Figs. 5 and 7. Additionally we compared our expressions for the case of $t = 0$, where we recover the results presented in Ref. [5]. The effect of the increase of the SOC leads to a, although small, decrease in the isotropic interaction but an increase in every anisotropic interaction and specially in the DMI, which now is the strongest interaction in the system. The main properties of each interaction does not present mayor changes in upon increasing the SOC, however, the isotropic component of the damping presents a strong shift in the local maxima, while the anisotropic component only intensify the

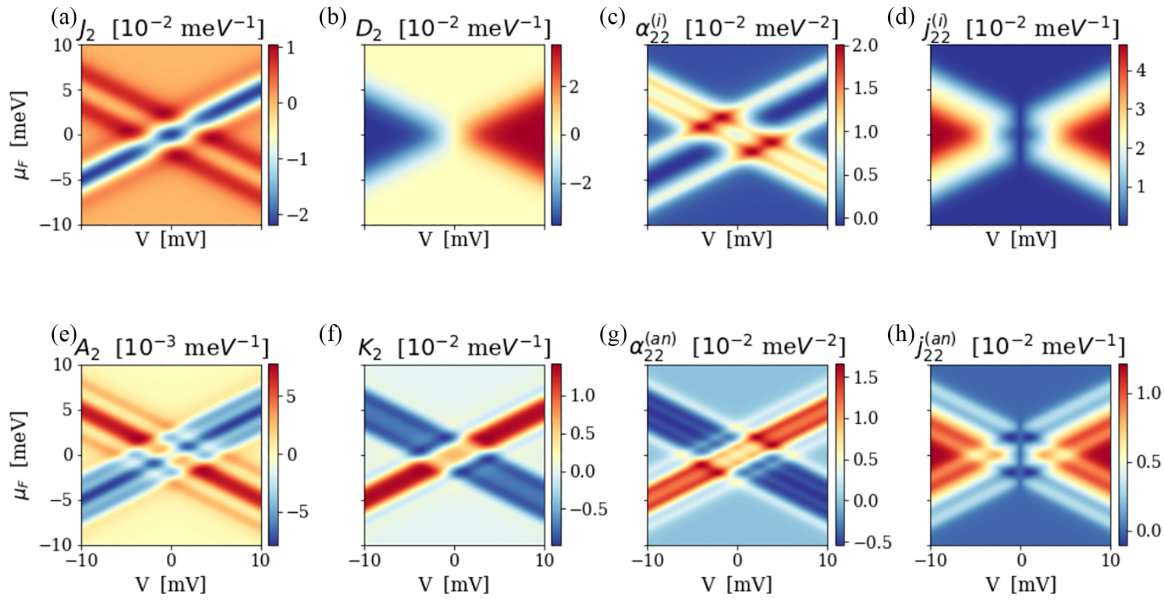

FIG. 7. Selected voltage-induced effective magnetic interactions and damping coefficient of the spin dimer. The increase of the SOC, presents a decrease of the symmetric interaction J_2 (a) by a factor of 2 but it still presents both positive and negative values, therefore inducing a ferromagnetic and antiferromagnetic configuration. However, for this case, the DMI (b) is now the dominant interaction preserving the steplike behavior. Similar increase can be seen with the anisotropic interactions A_2 (e) and K_2 (f). The effective Gilbert damping (c) shows the biggest change since now we can see how sensitive are the local maxima to the value of the SOC. The anisotropic damping (g) is now as relevant as the isotropic damping, and it also present a significant region were it injects energy. The isotropic (d) and anisotropic (h) components of the correlation function are now of the same order and eve preserve the structure with a bigger splitting of the local maxima from the SOC.

dependence in the extra local maxima lines. This clearly shows that not all lines are important for all effective terms and a proper analytical characterization is in order to understand the microscopical origin. Analogously to the interactions, the isotropic damping decreases while the anisotropic damping increases their value with an increase of the SOC. For the correlation functions, we see a similar behavior in terms of increase/decrease, but now both factors decrease the steepness of the steplike behavior and the relevance of the extra local maxima in the anisotropic factor.

As we can see in Fig. 5, due to the dominance of the DMI, the equilibrium orientation for the free spin goes from an antiparallel to an orthogonal configuration, related to the pinned spin, as we increase the bias voltage. Moreover, the unpinned spin have different directions ($\pm\hat{y}$) according to different signs of the bias voltage ($\sim \pm 3$ [mV]), and aside from a small deviation due to the symmetric interaction, the equilibrium orientations around $\pm\hat{y}$, in contrast with the weak SOC case, are sufficiently stable under small changes in the bias voltage. This opens the possibility to more exotic behaviors in a longer chain. However, the antiparallel configuration at $V = 0$ mV is preserved, which is expected since from the symmetries of the system we know that $D(V = 0) \equiv 0$. This case is specially interesting to test the limitations and/or validity of the approximate solution of the FP equation, since the conditions are related to the relation between the isotropic and anisotropic damping and correlation functions. In Fig. 5, we can see that even though the FP solution is not as reliable as in Fig. 4, the difference are very subtle and the characteristic parts are well represented.

[1] E. Moreno-Pineda and W. Wernsdorfer, Measuring molecular magnets for quantum technologies, Nat. Rev. Phys. **3**, 645 (2021).

[2] A. Aggarwal, V. Kaliginedi, and P. K. Maiti, Quantum circuit rules for molecular electronic systems: where are we headed based on the current understanding of quantum interference, thermoelectric, and molecular spintronics phenomena? Nano Lett. **21**, 8532 (2021).

[3] D. Gatteschi, R. Sessoli, and J. Villain, *Molecular Nanomagnets* (Oxford University Press on Demand, 2006), Vol. 5

[4] A. S. Núñez and R. A. Duine, Effective temperature and gilbert damping of a current-driven localized spin, Phys. Rev. B **77**, 054401 (2008).

[5] S. Díaz and Á. S. Núñez, Current-induced exchange interactions and effective temperature in localized moment systems, J. Phys.: Condens. Matter **24**, 116001 (2012).

[6] J. Rammer, *Quantum Field Theory of Non-Equilibrium States* (Cambridge University Press Cambridge, 2007), Vol. 22.

[7] M. O. A. Ellis, R. F. L. Evans, T. A. Ostler, J. Barker, U. Atxitia, O. Chubykalo-Fesenko, and R. W. Chantrell, The landau–lifshitz equation in atomistic models, Low Temp. Phys. **41**, 705 (2015).

[8] J.-X. Zhu, Z. Nussinov, A. Shnirman, and A. V. Balatsky, Novel Spin Dynamics in a Josephson Junction, Phys. Rev. Lett. **92**, 107001 (2004).

[9] J.-X. Zhu and J. Fransson, Electric field control of spin dynamics in a magnetically active tunnel junction, J. Phys.: Condens. Matter **18**, 9929 (2006).

[10] J. Fransson and J.-X. Zhu, Spin dynamics in a tunnel junction between ferromagnets, New J. Phys. **10**, 013017 (2008).

[11] P. Mondal, A. Suresh, and B. K. Nikolić, When can localized spins interacting with conduction electrons in ferro-or antiferromagnets be described classically via the landau-lifshitz equation: Transition from quantum many-body entangled to quantum-classical nonequilibrium states, Phys. Rev. B **104**, 214401 (2021).

[12] S.-H. Yang, R. Naaman, Y. Paltiel, and S. S. Parkin, Chiral spintronics, Nat. Rev. Phys. **3**, 328 (2021).

[13] Z. Shang, T. Liu, Q. Yang, S. Cui, K. Xu, Y. Zhang, J. Deng, T. Zhai, and X. Wang, Chiral-molecule-based spintronic devices, Small **18**, 2203015 (2022).

[14] A. J. Heinrich, W. D. Oliver, L. M. K. Vandersypen, A. Ardavan, R. Sessoli, D. Loss, A. B. Jayich, J. Fernandez-Rossier, A. Laucht, and A. Morello, Quantum-coherent nanoscience, Nat. Nanotechnol. **16**, 1318 (2021).

[15] B. Zeng, X. Chen, D.-L. Zhou, and X.-G. Wen, *Quantum Information Meets Quantum Matter: From Quantum Entanglement to Topological Phases of Many-Body Systems*, Quantum Science and Technology (Springer New York, New York, NY, 2019).

[16] M. Usman and K. Khan, Entanglement and multipartite quantum correlations in two-dimensional XY model with Dzyaloshinskii-Moriya interaction, Eur. Phys. J. D **74**, 181 (2020).

[17] H. Y. Yuan, Y. Cao, A. Kamra, R. A. Duine, and P. Yan, Quantum magnonics: When magnon spintronics meets quantum information science, Phys. Rep. **965**, 1 (2022).

[18] B. Zare Rameshti, S. Viola Kusminskiy, J. A. Haigh, K. Usami, D. Lachance-Quirion, Y. Nakamura, C.-M. Hu, H. X. Tang, G. E. Bauer, and Y. M. Blanter, Cavity magnonics, Phys. Rep. **979**, 1 (2022).

[19] S. A. Owerre, A first theoretical realization of honeycomb topological magnon insulator, J. Phys.: Condens. Matter **28**, 386001 (2016).

[20] R. Jaeschke-Ubiergo, E. Suarez Morell, and A. S. Nunez, Theory of magnetism in the van der Waals magnet CrI_3, Phys. Rev. B **103**, 174410 (2021).

[21] A. B. Cahaya and A. O. Leon, Dzyaloshinskii-moriya spin density by skew scattering, Phys. Rev. B **106**, L100408 (2022).

[22] G. Christou, D. Gatteschi, D. N. Hendrickson, and R. Sessoli, Single-molecule magnets, MRS Bull. **25**, 66 (2000).

[23] L. Bogani and W. Wernsdorfer, Molecular spintronics using single-molecule magnets, in *Nanoscience and Technology: A Collection of Reviews from Nature Journals* (World Scientific, 2010), pp. 194–201.

[24] S. J. Bartolome, F. Luis, and J. F. Fernández, *Molecular Magnets* (Springer, 2016).

[25] Z. Zhang, Y. Wang, H. Wang, H. Liu, and L. Dong, Controllable spin switching in a single-molecule magnetic tunneling junction, Nanoscale Res. Lett. **16**, 1 (2021).

[26] K. Biswas, M. Urbani, A. Sánchez-Grande, D. Soler-Polo, K. Lauwaet, A. Matěj, P. Mutombo, L. Veis, J. Brabec, K. Pernal *et al.*, Interplay between π-conjugation and exchange magnetism in one-dimensional porphyrinoid polymers, J. Am. Chem. Soc. **144**, 12725 (2022).

[27] C. de Graaf and R. Broer, *Magnetic Interactions in Molecules and Solids* (Springer International Publishing, 2016).

[28] H. Yang, S. O. Valenzuela, M. Chshiev, S. Couet, B. Dieny, B. Dlubak, A. Fert, K. Garello, M. Jamet, D.-E. Jeong *et al.*, Two-dimensional materials prospects for non-volatile spintronic memories, Nature **606**, 663 (2022).

[29] D. Ranieri, F. Santanni, A. Privitera, A. Albino, E. Salvadori, M. Chiesa, F. Totti, L. Sorace, and R. Sessoli, An exchange coupled meso-meso linked vanadyl porphyrin dimer for quantum information processing, Chem. Sci. **14**, 61 (2023).

[30] N. Friedrich, R. E. Menchón, I. Pozo, J. Hieulle, A. Vegliante, J. Li, D. Sánchez-Portal, D. Peña, A. Garcia-Lekue, and J. I. Pascual, Addressing electron spins embedded in metallic graphene nanoribbons, ACS Nano, **16**, 9 (2022).

[31] M. Mannini, F. Pineider, P. Sainctavit, C. Danieli, E. Otero, C. Sciancalepore, A. M. Talarico, M.-A. Arrio, A. Cornia, D. Gatteschi *et al.*, Magnetic memory of a single-molecule quantum magnet wired to a gold surface, Nat. Mater. **8**, 194 (2009).

[32] A. A. Khajetoorians, J. Wiebe, B. Chilian, and R. Wiesendanger, Realizing all-spin–based logic operations atom by atom, Science **332**, 1062 (2011).

[33] D. Pister, K. Irländer, D. Westerbeck, and J. Schnack, Toroidal magnetic molecules stripped to their basics, Phys. Rev. Res. **4**, 033221 (2022).

[34] Y.-X. Wang, Y. Ma, J.-S. Wang, Y. Yang, Y.-N. Guo, Y.-Q. Zhang, K.-J. Jin, Y. Sun, and P. Cheng, Ferroelectric single-molecule magnet with toroidal magnetic moments, Adv. Sci. **9**, 2202979 (2022).

[35] S. Wagner, F. Kisslinger, S. Ballmann, F. Schramm, R. Chandrasekar, T. Bodenstein, O. Fuhr, D. Secker, K. Fink, M. Ruben *et al.*, Switching of a coupled spin pair in a single-molecule junction, Nat. Nanotechnol. **8**, 575 (2013).

[36] J. Fransson, J. Ren, and J.-X. Zhu, Electrical and Thermal Control of Magnetic Exchange Interactions, Phys. Rev. Lett. **113**, 257201 (2014).

[37] T. Saygun, J. Bylin, H. Hammar, and J. Fransson, Voltage-induced switching dynamics of a coupled spin pair in a molecular junction, Nano Lett. **16**, 2824 (2016).

[38] R. Hanson, L. P. Kouwenhoven, J. R. Petta, S. Tarucha, and L. M. K. Vandersypen, Spins in few-electron quantum dots, Rev. Mod. Phys. **79**, 1217 (2007).

[39] K. X. Tran, A. S. Bracker, M. K. Yakes, J. Q. Grim, and S. G. Carter, Enhanced Spin Coherence of a Self-Assembled Quantum Dot Molecule at the Optimal Electrical Bias, Phys. Rev. Lett. **129**, 027403 (2022).

[40] D. Serrate, P. Ferriani, Y. Yoshida, S.-W. Hla, M. Menzel, K. Von Bergmann, S. Heinze, A. Kubetzka, and R. Wiesendanger, Imaging and manipulating the spin direction of individual atoms, Nat. Nanotechnol. **5**, 350 (2010).

[41] H. Katsura, A. V. Balatsky, Z. Nussinov, and N. Nagaosa, Voltage dependence of landau-lifshitz-gilbert damping of spin in a current-driven tunnel junction, Phys. Rev. B **73**, 212501 (2006).

[42] S. Bhattacharjee, L. Nordström, and J. Fransson, Atomistic Spin Dynamic Method with both Damping and Moment of Inertia Effects Included from First Principles, Phys. Rev. Lett. **108**, 057204 (2012).

[43] A. Płomińska and I. Weymann, Pauli spin blockade in double molecular magnets, Phys. Rev. B **94**, 035422 (2016).

[44] A. Palii, S. Aldoshin, B. Tsukerblat, J. M. Clemente-Juan, A. Gaita-Ariño, and E. Coronado, Electric field controllable magnetic coupling of localized spins mediated by itinerant electrons: a toy model, Phys. Chem. Chem. Phys. **19**, 26098 (2017).

[45] J. V. Jaramillo and J. Fransson, Charge transport and entropy production rate in magnetically active molecular dimer, J. Phys. Chem. C **121**, 27357 (2017).

[46] A. O. Leon, J. d'Albuquerque e Castro, J. C. Retamal, A. B. Cahaya, and D. Altbir, Manipulation of the rkky exchange by voltages, Phys. Rev. B **100**, 014403 (2019).

[47] K. Katcko, E. Urbain, B. Taudul, F. Schleicher, J. Arabski, E. Beaurepaire, B. Vileno, D. Spor, W. Weber, D. Lacour *et al.*, Spin-driven electrical power generation at room temperature, Commun. Phys. **2**, 116 (2019).

[48] Y.-J. Li, L.-Y. Chen, Y.-H. Xia, J.-M. Zhao, Y.-Q. Mu, G.-P. Zhang, and Y. Song, Designing multifunctional single-molecule devices by mononuclear or binuclear manganese phthalocyanines, Phys. E **134**, 114896 (2021).

[49] Y. Lu, Y. Wang, L. Zhu, L. Yang, and L. Wang, Electric field tuning of magnetic states in single magnetic molecules, Phys. Rev. B **106**, 064405 (2022).

[50] A. S. Núñez and A. H. MacDonald, Theory of spin transfer phenomena in magnetic metals and semiconductors, in *Foundations Of Quantum Mechanics In The Light Of New Technology: ISQM–Tokyo'05* (World Scientific, 2006), pp. 150–158.

[51] R. A. Duine, A. S. Núñez, J. Sinova, and A. H. MacDonald, Functional keldysh theory of spin torques, Phys. Rev. B **75**, 214420 (2007).

[52] C. Kittel and P. McEuen, *Introduction to Solid State Physics* (Wiley New York, 1976), Vol. 8.

[53] R. Winkler, *Spin-Orbit Coupling Effects in Two-Dimensional Electron and Hole Systems*, Springer Tracts in Modern Physics (Springer, New York, NY, 2003).

[54] J. Birkholz and V. Meden, Spin–orbit coupling effects in one-dimensional ballistic quantum wires, J. Phys.: Condens. Matter **20**, 085226 (2008).

[55] S. Brinker, M. dos Santos Dias, and S. Lounis, Generalization of the landau–lifshitz–gilbert equation by multi-body contributions to gilbert damping for non-collinear magnets, J. Phys.: Condens. Matter **34**, 285802 (2022).

[56] J. Fujimoto, Field theoretical approach to spin torques: Slonczewski torques, arXiv:2208.09581.

[57] A. Manchon and S. Zhang, Theory of spin torque due to spin-orbit coupling, Phys. Rev. B **79**, 094422 (2009).

[58] H. Risken, Fokker-planck equation, in *The Fokker-Planck Equation* (Springer, 1996), pp. 63–95.

[59] A. Spinelli, B. Bryant, F. Delgado, J. Fernández-Rossier, and A. F. Otte, Imaging of spin waves in atomically designed nanomagnets, Nat. Mater. **13**, 782 (2014).

[60] A. Auerbach, *Interacting Electrons and Quantum Magnetism* (Springer Science & Business Media, 2012).

[61] J. W. Negele, *Quantum Many-Particle Systems* (CRC Press, 2018).

[62] S. Datta, *Electronic Transport in Mesoscopic Systems* (Cambridge University Press, 1997).

[63] S. Datta, *Quantum Transport: Atom to Transistor* (Cambridge University Press, 2005).